

# Improved stability predictions in milling through more realistic load conditions

**Conference Paper****Author(s):**

Postel, Martin; Bugdayci, Nevzat B.; Monnin, Jérémie; Kuster, Friedrich; Wegener, Konrad

**Publication date:**

2018

**Permanent link:**

<https://doi.org/10.3929/ethz-b-000306899>

**Rights / license:**

[Creative Commons Attribution-NonCommercial-NoDerivatives 4.0 International](#)

**Originally published in:**

Procedia CIRP 77, <https://doi.org/10.1016/j.procir.2018.08.231>

8th CIRP Conference on High Performance Cutting (HPC 2018)

# Improved stability predictions in milling through more realistic load conditions

Postel<sup>a</sup> M.\*, Bugdayci<sup>a</sup> N.B., Monnin<sup>b</sup> J., Kuster<sup>a</sup> F., Wegener<sup>a</sup> K.

<sup>a</sup> Institute of Machine Tools and Manufacturing (IWF), ETH Zurich, Switzerland

<sup>b</sup> Mikron AgieCharmilles AG, Ipsachstrasse 16, 2560 Nidau, Switzerland

\* Corresponding author. Tel.: +41 44 632 94 45; fax: +41 0 44 632 1125. E-mail address: [postel@iwf.mavt.ethz.ch](mailto:postel@iwf.mavt.ethz.ch)

## Abstract

In this paper, the combined influence of the load condition and the spindle speed on the tooltip dynamics of a five-axis milling machine with dominant spindle modes is evaluated. A constant preload is applied through axially and radially arranged permanent magnets while the dynamic excitation of the rotating dummy tool takes place by a force impact. The structures response is measured with non-contact sensors and Frequency Response Functions (FRFs) are calculated. The required load levels are derived from time domain simulation of the process. The so-obtained stability charts are hence functions of the rotational speed and the load condition which in turn depends on the feed rate and depth of cut. For validation, cutting tests are performed in Aluminum 7075 and results are compared against the predicted lobes. The stability boundary resulting from this approach is capable to explain the shift of the stability pocket which is observed in the cutting experiments when comparing different feed rates.

© 2018 The Authors. Published by Elsevier Ltd.

This is an open access article under the CC BY-NC-ND license (<https://creativecommons.org/licenses/by-nc-nd/4.0/>)

Selection and peer-review under responsibility of the International Scientific Committee of the 8th CIRP Conference on High Performance Cutting (HPC 2018).

*Keywords:* Chatter stability; Frequency Response Function; Nonlinearity; Load dependency

## 1. Introduction

Regenerative chatter remains the main limiting factor in milling operations. The most common approach to differentiate stable from unstable cutting conditions is the creation of stability lobe diagrams [1]. This approach requires the dynamics at the tooltip which are usually measured at standstill of the machine. However, it is well known that the dynamics of a machine may change at high spindle speeds [2-4]. Then, centrifugal forces and gyroscopic moments play an important role for bearing characteristics and shaft dynamics and hence the overall TCP dynamics [5]. A rise in temperature can also have significant effects as thermal expansion may change the preload of the bearings [6, 7]. Additionally, some spindles perform speed-dependent preload adjustments which may also lead to changes in natural frequency and damping ratios when compared to

measurements at standstill [8]. Moreover, it has been observed that the load condition can influence the resulting dynamics as well [9].

However, while extensive studies have been performed on the speed dependent behavior of spindles and some work also exists on the influence of the load condition, little research has been conducted on the combined effect of spindle speed, preload and excitation level on TCP dynamics and on the resulting stability boundary.

The aim of the present work is to investigate the interaction between applied loads and spindle speed and to show its importance for the creation of feed and depth of cut dependent stability charts when the dominant modes are modes of the spindle system. A specifically designed setup is used and after investigation of the isolated factors the approach is applied to the creation of speed and load dependent stability charts.

## 2. Background

### 2.1. Characterization of machine tool dynamics

Typically, the dynamics of a machine tool are investigated with the help of an instrumented impulse hammer. While this is a convenient way to characterize the dynamics of a structure, its major drawback is that the type of excitation differs significantly from a real cutting process.

In this work, the cutting process is considered as a superposition of a constant preload on the one hand and dynamic force components on the other. While replicating the acting preload during impact testing is straightforward, the different types of excitation make it less obvious how the dynamic cutting force and the force impact are correlated. In order to still be able to qualitatively compare the two quantities, the power and energy of a process as defined in signal processing are introduced first.

### 2.2. Cutting process

A stable cutting process is a stationary process for which the power spectral density can be estimated through the Fast Fourier Transform (FFT) of a signal  $x$  as

$$\tilde{S}_{xx}[k] = \frac{\Delta t}{N} |X_k|^2. \quad (1)$$

In there,  $X_k$  is the Discrete Fourier Transform of signal  $x$  that was sampled at points  $x_k = x[k\Delta t]$  with  $k = 0 \dots N - 1$ .

The average power  $P$  can be obtained by summing over all frequencies and multiplying with the frequency bin width  $\Delta f$ ,

$$P = \Delta f \cdot \sum_{k=0}^{N-1} \tilde{S}_{xx}[k]. \quad (2)$$

In the following, power only refers to the power of the dynamic component of the cut, i.e. the power spectral density is calculated from the force signal with its constant component subtracted. This yields two principal quantities per Cartesian direction that are used to define a given cut: The static preload  $F_s$  and the power of the dynamic component  $P$ .

When a linear cutting force model is assumed, the following relations between feed per tooth  $f_t$  and depth of cut  $a_p$ , and static load and power of the cut hold:

$$F_s \propto f_t, a_p, \quad P \propto f_t^2, a_p^2. \quad (3)$$

Usually, the FRFs are assumed to be independent of the load case, i.e.  $FRF \neq f(F_s, P)$ , and one set of measurements can be used for stability predictions under any cutting condition. However, the stability boundary must be found iteratively in cases where this assumption is violated. While e.g. stability calculations using a FRF obtained under load conditions present at 1.0 mm depth of cut might suggest that 1.5 mm is the stability limit, stability calculations using FRFs that were performed under conditions present at 1.5 mm lead

to a limit of 1.7 mm. This process is repeated until the predicted stability limit is lower than the depth of cut which was used to derive the load conditions for the respective experiment. This is the actual critical depth of cut for that specific spindle speed and the so obtained stability limit is later referred to as the “adapted” stability limit.

### 2.3. Impact testing

Different from the cutting process, an impact hammer produces an impulse-like force signal of finite duration  $T_f$ . For such signals, it is more suitable to define the energy  $E$ , again as defined in signal processing,

$$E = \sum_{k=0}^{N-1} |x[k\Delta t]|^2 \quad (4)$$

where  $T_f = (N - 1) \cdot \Delta t$ . The quantities in Eqs. (2) and (4) cannot be compared on an absolute scale. Still, the assumption is made that a relative comparison is possible: If the power of the cutting process is doubled, also the energy of the impact should be doubled. In Chapter 4 details about a possible approach for correlation of the two quantities are presented.

## 3. Experimental setup

The experimental setup for the investigation of machine dynamics under load and spindle speed is shown in Fig. 1.

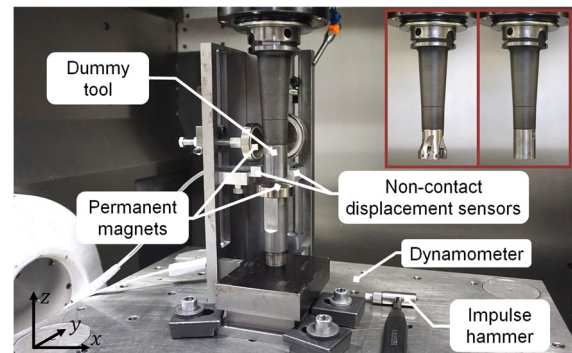


Fig. 1. Experimental setup. The figures in the top right corner show the five inserts cutter used in the cutting experiments, compared against the dummy tool that is used for the rotating impact tests.

A fixture is designed to which the permanent magnets as well as the non-contact sensors can be mounted. The fixture is screwed on a tabletop dynamometer such that the applied constant forces can be measured. To adjust the constant forces, the magnets can be moved with a screw in axial and radial direction, respectively.

A cylindrical tool is necessary to investigate spindle speed dependent FRFs. The dummy tool shown in Fig. 1 replaces a five inserts cutter of the same mass and approximately same stiffness. This leads to the TCP dynamics of artifact and actual tool being almost identical. The rotating dummy tool is impacted and the response is measured. Prior to FRF calculation, the spindle speed synchronous content is removed using the time-domain based approach presented in [10].

## 4. Experimental results

In the following, sample experimental results are presented. All tests are performed on a Mikron high performance five-axis milling machine and the tool shown in Fig. 1 is used.

### 4.1. Parameter study

First, the distinct influences of axial and radial preload and energy of the force impact are investigated. Along with 0 rpm, three different spindle speeds are investigated: 3000, 9000 and 13000 rpm. Prior to every experiment, a warm up cycle is run to minimize thermal influences. In the following three tests, the impact energy is kept between  $1 \cdot 10^5$  and  $5 \cdot 10^5 \text{ N}^2$ .

### Influence of spindle speed

Fig. 2 summarizes the behavior of the TCP dynamics in x- and y-direction with changing spindle speed. It can be seen that the modes in the low frequency region (up to  $\sim 300$  Hz, modes of the machine tool) and the ones around 1400 Hz are barely affected by the change in speed. On the other hand, the modes around 700 Hz and 1000 Hz are very sensitive to speed variation.

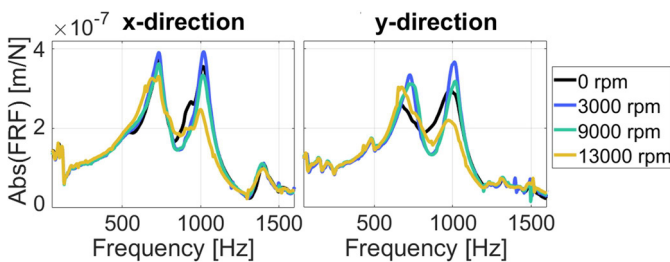


Fig. 2. Measured FRFs as a function of spindle speed.

### Influence of axial preload

Fig. 3 shows the FRFs obtained for different axial preloads at standstill and 13000 rpm. For both spindle speeds, a significant change of the mode at 1000 Hz can be observed. However, the behavior at 0 rpm and 13000 rpm is quite different. While for 0 rpm the mode mostly shifts to a lower frequency and slightly decreases in amplitude with increasing load, for 13000 rpm it completely vanishes under the highest preload. This observation stresses the importance of considering the combined effect of spindle speed and axial load.

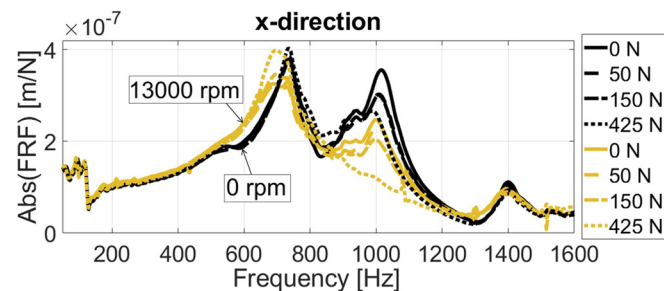


Fig. 3. Measured FRFs in x-direction for different axial preloads at 0 rpm and 13000 rpm. Results in y-direction are similar and not depicted here.

### Influence of radial preload

In the next experiment a constant radial preload is applied in x- and y-direction while the rotating dummy is impacted. Fig. 4 shows the measured FRFs for spindle speeds of 9000 and 13000 rpm with radial loads between 0 and 400 N. For all spindle speeds only a minor influence can be observed.

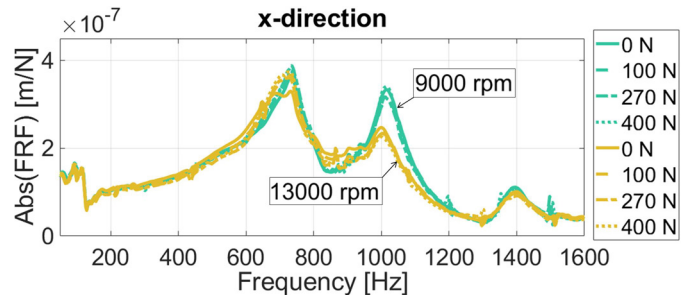


Fig. 4. Measured FRFs for different radial preloads at 9000 and 13000 rpm.

### Influence of impact energy

In this setup, no constant preload is applied. Instead, impacts are performed with different impact energies. In total, between 150 and 250 impacts are performed for each spindle speed and are then grouped according to their energy content, see Fig. 5. Again, the mode around 1000 Hz starts to merge with the one around 700 Hz with increasing force level. Note that the modes at 100 and 1400 Hz are basically unaffected.

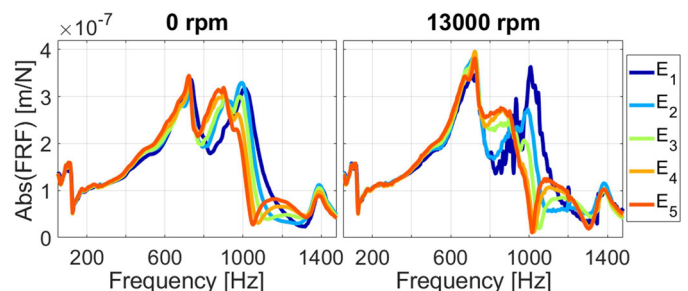


Fig. 5. Measured FRFs in x-direction at 0 rpm (left) and 13000 rpm (right) for different impact energy levels:  $E_1 = 0 \dots 3 \cdot 10^6 \text{ N}^2$ ,  $E_2 = 3 \dots 6 \cdot 10^6 \text{ N}^2$ ,  $E_3 = 6 \dots 9 \cdot 10^6 \text{ N}^2$ ,  $E_4 = 9 \dots 12 \cdot 10^6 \text{ N}^2$ ,  $E_5 = 12 \dots 15 \cdot 10^6 \text{ N}^2$ .

### 4.2. Case study

The strategy of creating preload and cutting power dependent stability lobes is now applied to a real cutting process. The five inserts cutter shown in Fig. 1 is used for a slotting operation in Aluminum 7075. Feed rates are chosen as 0.03, 0.08 and 0.15 mm/tooth. Cutting coefficients are identified at 9000 rpm using the mechanistic approach. The load conditions for different depths of cut and feed rates are derived from time domain simulations where a rigid tool is assumed. Calculated preloads and power in each direction are shown in Fig. 6. As described, the calculated preload is simply applied with permanent magnets. However, it is not immediately clear how the energy of the impact in x- and y-direction can be correlated with the power of the force signals.

Here, the inverse approach is taken: Using the chatter frequencies obtained at 2.5 mm for 9000 rpm at feed  $f_t = 0.08$  mm/tooth, the FRFs that match the experimental

results best are chosen as the reference FRFs. The energies of the respective impacts are  $9 \cdot 10^5$  and  $3.1 \cdot 10^6$  N<sup>2</sup> while the corresponding power in the cut is 108 N<sup>2</sup> and 380 N<sup>2</sup> in x- and y-direction, respectively. For all subsequent depths of cut and feed rates of interest the impact energy is scaled according to this reference energy. For the highest feed rate, the calculated impact energy at 3.5 and 4.0 mm depth of cut could not be achieved with the hammer available.

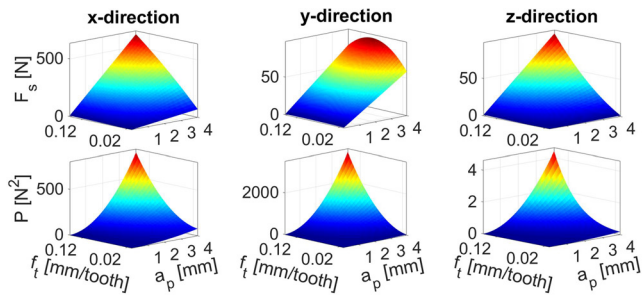


Fig. 6. Static load  $F_s$  and Power  $P$  as a function of depth of cut  $a_p$  and feed  $f_t$

For more robust results in the cutting experiments, each cutting condition is repeated between three and five times. Results for the three different feed rates along with the predictions at the different depths of cut are shown in Fig. 7.

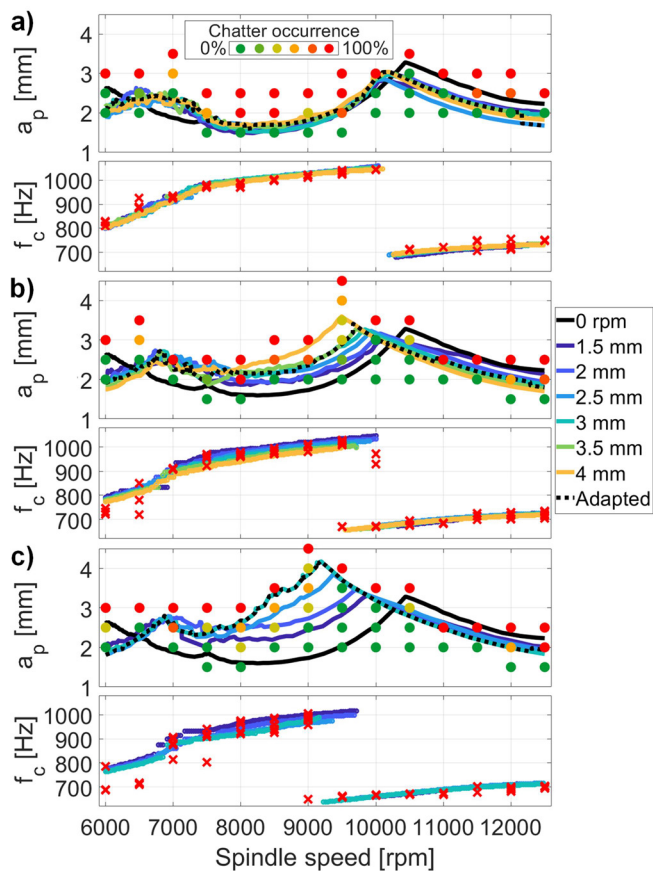


Fig. 7. Predicted speed and load dependent stability diagrams and chatter frequencies for a) 0.03 mm/tooth, b) 0.08 mm/tooth and c) 0.15 mm/tooth. The 0 rpm stability lobe is calculated from FRF measurements at idle state with impact energies of  $1 \dots 5 \cdot 10^5$  N<sup>2</sup>. The adapted prediction is the iteratively found critical depth of cut following the procedure described in Section 2.2.

It can be seen that the load dependent stability charts are able to explain most of the shift of the stability lobe that occurs at 9000 rpm for higher feed rates. Also, the feed dependent chatter frequencies are predicted much more accurately with this approach.

### 5. Conclusion

An experimental setup was presented that allows investigating the combined influence of load and spindle speed on the TCP dynamics of a milling machine. Results showed that especially the axial load can play a significant role for natural frequency and damping of spindle-related modes. Also, it is important to note that this influence can be very different at different spindle speeds. For a given process the main factors contributing to a change in the load condition are the feed rate, immersion angles and depth of cut. The dependency on the depth of cut leads to a process in which the actual critical depth of cut has to be found iteratively. This approach was successfully applied to a milling process.

The main issue that remains is finding a more reliable approach to establish a relationship between the necessary energy of the impact and the power of the cutting process. This problem is still under investigation.

### Acknowledgements

The authors would like to thank the Commission for Technology and Innovation (CTI) of the Federal Department of Economic Affairs of Switzerland for the financial support.

### References

- [1] Altintas Y, Budak E. Analytical Prediction of Stability Lobes in Milling. *CIRP Annals - Manufacturing Technology* 1995;44(1):357-362.
- [2] Ozsahin O, Budak E, Ozguven HN. In-process tool point FRF identification under operational conditions using inverse stability solution. *International Journal of Machine Tools & Manufacture* 2015;89:64-73.
- [3] Faassen RPH, van de Wouw N, Oosterling JAJ. Prediction of regenerative chatter by modelling and analysis of high-speed milling. *International Journal of Machine Tools and Manufacture* 2013;43(14):1437-1446.
- [4] Grossi N, Montevecchi F, Sallèse L, Scippa A, Campatelli G. Chatter stability prediction for high-speed milling through a novel experimental-analytical approach. *International Journal of Advanced Manufacturing Technology* 2017;89:2587-2601.
- [5] Cao H, Li B, He Z. Chatter stability of milling with speed-varying dynamics of spindles. *International Journal of Machine Tools and Manufacture* 2012;52(1):50-58.
- [6] Gao SH, Meng G, Long XH. Stability prediction in high-speed milling including the thermal preload effects of bearing. *Proceedings of the Institution of Mechanical Engineers, Part E: Journal of Process Mechanical Engineering* 2009;224(1):11-22.
- [7] Delgado AS, Ozturk E, Sims N. Analysis of Non-linear Machine Tool Dynamic Behavior. *Procedia Engineering* 2013; 63(Suppl. C):761-770.
- [8] Ozturk E, Kumar U, Turner S, Schmitz T. Investigation of spindle bearing preload on dynamics and stability limit in milling. *CIRP Annals* 2012;61(1):343-346.
- [9] Jamil N, Yusoff AR. Electromagnetic actuator for determining frequency response functions of dynamic modal testing on milling tool. *Measurement* 2016;82:355-366.
- [10] Cheng CH, Schmitz TL, Scott Duncan G. Rotating Tool Point Frequency Response Prediction Using Rcsa. *Machining Science and Technology* 2007;11(3):433-446.